ORIGINAL ARTICLE



Check for updates

Identification and characterization of novel MPC1 gene variants causing mitochondrial pyruvate carrier deficiency

Huafang Jiang¹ | Ahmad Alahmad^{2,3} | Song Fu^{4,5} | Xiaoling Fu⁶ | Zhimei Liu¹ | Xiaodi Han¹ | Lanlan Li⁵ | Tianyu Song¹ | Manting Xu¹ | Shanshan Liu^{4,5} | Junling Wang¹ | Buthaina Albash³ | Ahmad Alaqeel³ | Vasilescu Catalina^{7,8} | Holger Prokisch^{1,7,8} | Robert W. Taylor^{2,9} | Robert McFarland^{2,9} | Fang Fang¹

Correspondence

Fang Fang, Department of Neurology, Beijing Children's Hospital, Capital Medical University, National Center for Children's Health, Nanlishi Road No. 56, Xicheng District, Beijing 100045,

Email: fangfang@bch.com.cn

Funding information

Beijing Children's Hospital for Children Medication Foundation, Grant/Award Number: YZZD202001; Beijing Foreign High-level Talents Foundation Project, Grant/Award Number: G20200101021; Capital Health Research and Development of Special, Grant/Award Number: 2018-2-2096; PerMiM project, Grant/ Award Number: 01KU2016A; the China Association Against Epilepsy Scientific Research Project, Grant/Award Number: CX-B-2021-09; the Medical Research Council (MRC) International Centre for Genomic Medicine in Neuromuscular Disease, Grant/Award Number: MR/ S005021/1; the Mitochondrial Disease

Abstract

Pyruvate, the end product of glycolysis, is a key metabolic molecule enabling mitochondrial adenosine triphosphate synthesis and takes part in multiple biosynthetic pathways within mitochondria. The mitochondrial pyruvate carrier (MPC) plays a vital role in transporting pyruvate from the cytosol into the organelle. In humans, MPC is a hetero-oligomeric complex formed by the MPC1 and MPC2 paralogs that are both necessary to stabilize each other and form a functional MPC. MPC deficiency (OMIM#614741) due to pathogenic MPC1 variants is a rare autosomal recessive disease involving developmental delay, microcephaly, growth failure, and increased serum lactate and pyruvate. To date, two MPC1 variants in four cases have been reported, though only one with a detailed clinical description. Herein, we report three novel pathogenic MPC1 variants in six patients from three unrelated families, identified within European, Kuwaiti, and Chinese mitochondrial disease patient cohorts, one of whom presented as a Leigh-like syndrome. Functional analysis in primary fibroblasts from the patients revealed decreased expression of MPC1 and MPC2. We rescued pyruvate-driven oxygen consumption rate in patient's fibroblasts by reconstituting with wild-type MPC1. Complementing homozygous MPC1 mutant cDNA with CRISPR-deleted MPC1 C2C12 cells verified the

¹Department of Neurology, Beijing Children's Hospital, Capital Medical University, National Center for Children's Health, Beijing, China

²Wellcome Centre for Mitochondrial Research, Translational and Clinical Research Institute, Faculty of Medical Sciences, Newcastle University, Newcastle upon Tyne, UK

³Kuwait Medical Genetics Centre, Kuwait City, Kuwait

⁴Graduate School of Peking Union Medical College, Beijing, China

⁵National Institute of Biological Sciences, Beijing, China

⁶Department of Pediatrics, Guizhou Provincial People's Hospital, Guiyang, China

⁷Institute of Human Genetics, Technical University of Munich, Munich, Germany

⁸Institute of Human Genetics, Helmholtz Zentrum München, Munich, Germany

⁹NHS Highly Specialised Services for Rare Mitochondrial Disorders, Royal Victoria Infirmary, Newcastle upon Tyne Hospitals NHS Foundation Trust, Newcastle upon Tyne, UK

Patient Cohort, Grant/Award Number: G0800674; Wellcome Trust Centre for Mitochondrial Research, Grant/Award Number: 203105/Z/16/Z

Communicating Editor: Saskia Brigitte Wortmann mechanism of variants: unstable MPC complex or ablated pyruvate uptake activity. Furthermore, we showed that glutamine and beta-hydroxybutyrate were alternative substrates to maintain mitochondrial respiration when cells lack pyruvate. In conclusion, we expand the clinical phenotypes and genotypes associated with MPC deficiency, with our studies revealing glutamine as a potential therapy for MPC deficiency.

KEYWORDS

glutamine, Leigh-like syndrome, mitochondria, mitochondrial pyruvate carrier deficiency, *MPC1*, treatment

Synopsis

We report six cases of mitochondrial pyruvate carrier deficiency caused by deleterious *MPC1* variants and illustrate glutamine supplementation as a potential therapeutic strategy.

1 | INTRODUCTION

Mitochondrial pyruvate carrier (MPC) deficiency (OMIM#614741) is a rare autosomal recessive inherited metabolic disease caused by a defective MPC, which is located in the inner mitochondrial membrane. MPC transports pyruvate from the cytosol into the mitochondrial matrix, providing the primary substrate for the tricarboxylic acid (TCA) cycle, which further produces electron donors for oxidative phosphorylation (OXPHOS).¹ Mammalian MPC is a 150 kDa heterocomplex formed by MPC1 and MPC2 proteins, and it plays a pivotal role in energy metabolism.^{2,3} Both MPC1 and MPC2 are essential for each other's stability and for MPC complex formation.4 In 2003, Brivet et al.5 reported the first case of MPC deficiency that presented with developmental delay, mild facial dysmorphism, progressive microcephaly, and hyperlactataemia with a normal lactate/pyruvate ratio. The patient's brain MRI showed cerebral atrophy with evidence of ventricular dilatation, periventricular leucomalacia, and calcifications. The underlying genetic defect in the patient was identified in 2012 by Bricker and colleagues,² a homozygous c.289C > T (p.Arg97Trp) variant in MPC1, and recognized to be an essential component of MPC. Additionally, this landmark study included three other cases with homozygous c.236 T > A (p.Leu79His) variants in the same gene. To date, Bricker et al.'s² report remains the only report of MPC1 variants, with two pathogenic variants in four patients, and only one with a detailed clinical description. Moreover, no cases of MPC deficiency caused by MPC2 variant have been found.

Herein, we describe six additional cases from three unrelated families. Together, they harbour three novel pathogenic variants in *MPC1*, one patient (F1-I) has compound heterozygous variants and whereas the others (F2-I/II/III and F3-I/II) have homozygous variants. We

analysed the mechanism by which the *MPC1* variants decrease MPC function and investigated the underlying substrates that drive mitochondrial respiration when cells lack pyruvate. We summarize the clinical symptoms and cranial MRI findings in MPC deficiency and provide new clinical and pathophysiological insight into this disease, and our work also proposes glutamine as a potential treatment.

2 | METHODS

2.1 | Participants

We enrolled patients with bi-allelic recessive pathogenic variants in *MPC1* diagnosed by whole-exome sequencing (WES) from mitochondrial disease patient cohorts in Europe, Kuwait, and China. Six cases from three families (F1-I; F2-I, F2-II, and F2-III; F3-I and F3-II) were recruited in this study, and their pedigrees are shown in Figure 1. Families 1 and 3 were from China. Family 2 was from Kuwait.

2.2 | Whole-exome sequencing (WES)

Peripheral blood samples were collected from the patients and their families. WES was performed to detect causative genes using an Illumina HiSeq X Ten sequencer (Illumina, San Diego) for F1-I and F3-II, and Illumina NextSeq500 platform for F2-II. ANNOVAR software was used for variant filtering and annotation.⁶ For each variant, minor allele frequencies were checked in variant databases, including the 1000 Genomes,⁷ gnomAD,⁸ and Exome Aggregation

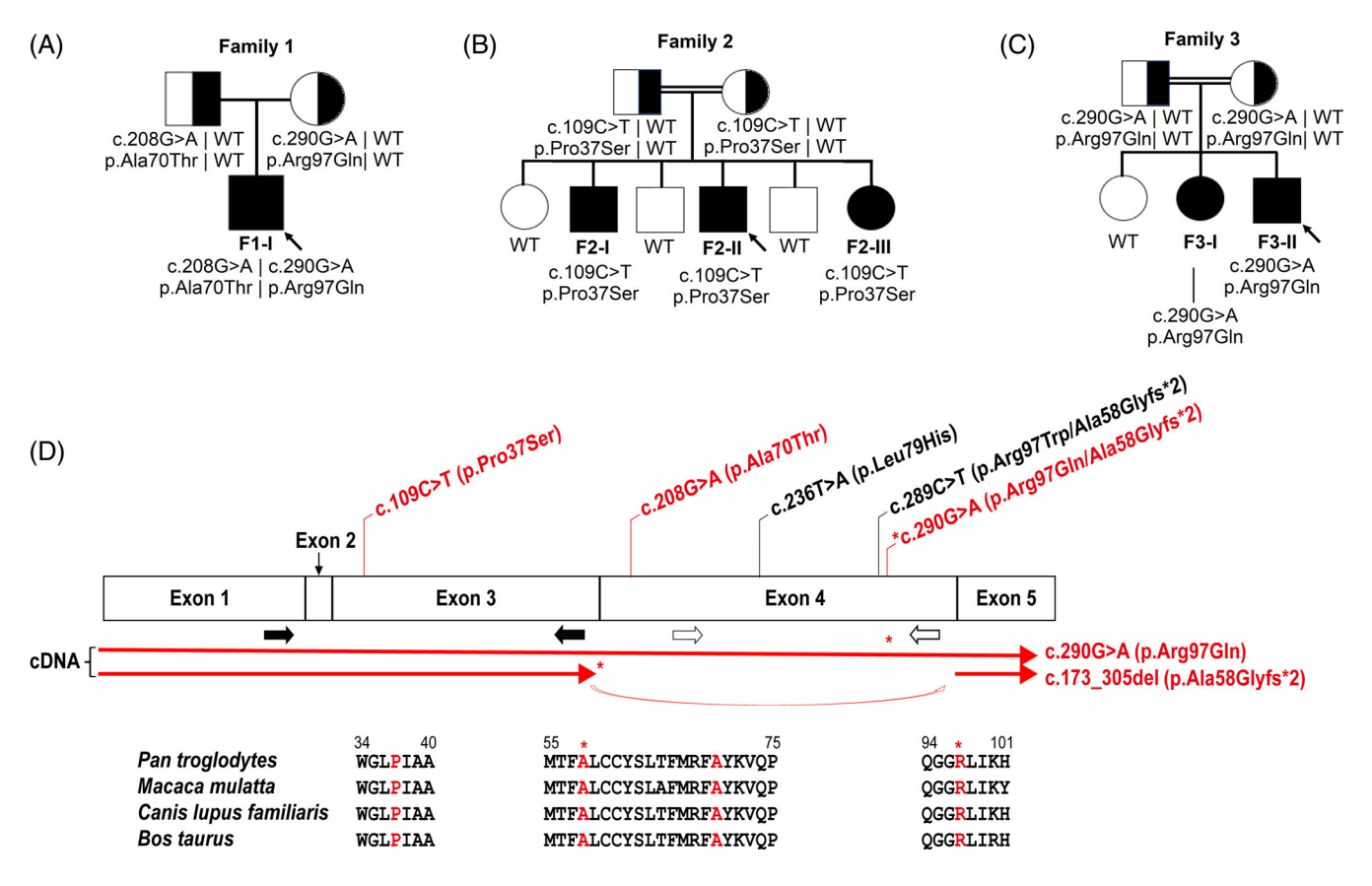


FIGURE 1 Genetic findings of the cases presented in this study. A-C, Pedigrees of family 1 (A), family 2 (B), and family 3 (C). D, Schematic diagram of MPC1 organization illustrates the locations of the variants identified in our report and previous studies. Variants discovered in our report are shown in red. The c.290G > A variant generates two mRNA transcripts shown as red arrows: a full-length transcript containing the point mutation (p.Arg97Gln) and a mis-spliced transcript (p.Ala58Glyfs*2) missing the entire exon 4. Amino acids substitutions caused by c.290G > A are marked by *. Black solid arrows indicate the location of qPCR primer pairs testing the total MPC1 mRNA expression, and open arrows correspond to the primers amplifying full-length MPC1 mRNA. Phylogenetic conservation among the affected amino acid residues is presented in the alignment of homologs across different species. qPCR, Quantitative polymerase chain reaction; WT, wild type

Consortium (ExAC)⁹ databases. Pathogenicity of identified variants was evaluated using multiple bioinformatics tools including SIFT,¹⁰ PolyPhen-2,¹¹ MutationTaster,¹² CADD,¹³ and PROVEAN.¹⁴ Variants were interpreted according to the guidelines published by ACMG.¹⁵ Sanger sequencing was conducted to confirm the presence of identified variants and that they segregated within the families. We had submitted all the variants mentioned in this article to ClinVar, and the accession numbers are SCV001934591, SCV001842675, and SCV001842676.

2.3 | MPC1 cDNA analysis

To test the effect of variants on *MPC1* transcripts, total RNA was extracted from cultured fibroblasts (F1-I) using TRIzol method and then reverse transcribed to cDNA using All-in-One First-Strand cDNA Synthesis Kit

(QP006, GeneCopoeia). Polymerase chain reaction (PCR) primers used to amplify the *MPC1* coding region (about 460 bp) are listed in Table S1. PCR products were separated on a 2% agarose gel, extracted, purified, and then sequenced.

2.4 | Real-time quantitative PCR (qRT-PCR) analysis of the expression of *MPC1* and *MPC2* genes

cDNA was synthesized from total RNA extracted from fibroblasts(F1-I). The relative levels of *MPC1* and *MPC2* mRNA were determined using SYBR Premix Ex Taq (RR820A, Takara) and CFX96 Touch Real-Time PCR Detection System (Bio-Rad). Sequence-specific primers are listed in Table S1. 16 Data were processed and normalized to β -actin according to the $2^{-\Delta\Delta ct}$ method.

2.5 | Cell culture

Primary dermal fibroblast cultures were generated from skin biopsies from the patients (F1-I, F2-I, and F2-II) and two healthy controls. Fibroblasts (F1-I) and C2C12 wild-type (WT) cells were grown in Dulbecco's Modified Eagle Medium (DMEM) supplemented with 4.5 g/L glucose, 10% fetal bovine serum (FBS), and 1% penicillin/streptomycin (PS). F2-I and F2-II fibroblasts were cultured with the addition of 1X non-essential amino acids and 50 µg/ml uridine. MPC1 knockout C2C12 cells ($\Delta MPC1$) were grown in DMEM supplemented with 4.5 g/L glucose, 10% FBS, 1% PS, 4 mM L-glutamine, 3 mM sodium pyruvate, 50 µg/ml uridine, and 1 mM citrate. Cells were maintained at 37°C in a humidified 5% CO₂ atmosphere.

2.6 | MPC1 knockout in C2C12 cells

CRISPR sgRNAs targeting exons 3 and 4 of MPC1 were subcloned into PX458 plasmids (48 138, Addgene) at BbsI, as previously described. The sgRNA sequences were 5'-CACCGTCTG GGGCCCAGTTGCCAAC-3' and 5'-CACCGATTCATGAG ATTTGCCTACA-3'. Plasmids expressing the sgRNAs were transfected into C2C12 cells using polyethylenimine (BMS1003, ThermoFisher Scientific), and GFP positive cells were sorted in 96-well plates to generate a stable $\Delta MPC1$ cell line. MPC1 knockout cells were confirmed using western blots.

2.7 | Genetic complementation of fibroblasts and $\Delta MPC1$ cell lines

For genetic complementation, cDNA containing p. Ala58Glyfs*2 was derived from patient (F1-I) fibroblasts. The cDNAs expressing human MPC1 WT and MPC1 variants (p.Ala70Thr and p.Arg97Gln) were assembled with pcDNA3.1+ vector (V79020, ThermoFisher Scientific) and then subcloned into a FUIPW lentiviral vector. Plasmids used in this study (Table S1) were generated using the Gibson assembly method.¹⁸ Viruses were produced by packaging pMD2.G (12 259, Addgene) and psPAX2 (12 260, Addgene) vectors in HEK293T cells, as published previously. 19 Fibroblasts (F1-I) were transduced with a lentivirus expressing MPC1 WT protein using 8 µg/ml polybrene (TR-1003, Sigma-Aldrich), and ΔMPC1 cell lines were transduced with lentiviruses expressing MPC1 WT and mutated proteins (Ala70Thr, Arg97Gln, and Ala58Glyfs*2). Transduced cells were selected by incubation with 20 µg/ml puromycin (A1113803, ThermoFisher Scientific) for 4 days and maintained without puromycin.

Western blots were used to detect protein expression to identify cells where complementation occurred.

2.8 | Western blot

Protein (25-50 μg) from fibroblasts (F1-I, F2-I, and F2-II) and C2C12 cells were electrophoresed on sodium dodecyl sulfate-polyacrylamide gel electrophoresis gels. Immunoblotting was performed with primary antibodies as follows: anti-MPC1 (14 462, Cell Signaling Technology), anti-MPC2 (46 141, Cell Signaling Technology), Total OXPHOS Human WB Antibody Cocktail (consisting of five antibodies: anti-ATP5A, -UQCRC2, -SDHB, -COXII, and -NDUFB8; ab110411, Abcam), anti-SDHA (ab14715, Abcam), anti-ATP5A (ab14748, Abcam), anti-CORE2 (ab14745, Abcam), anti-COX2 (ab110258, Abcam), anti-NDUFB8 (ab110242, Abcam), and anti-β-actin (3700, Cell Signaling Technology). All protein experiments were repeated at least three times, and the density of each band was quantified using ImageJ software (National Institutes of Health).

2.9 | Mitochondrial respiration

The oxygen consumption rate (OCR) in fibroblasts (F1-I) was assessed with the XF96 Extracellular Flux Analyzer (Agilent) using 20 000 cells per well, as previously described.²⁰ Before measuring respiration, culture medium was replaced with XF Base Medium Minimal DMEM (102353-100, Agilent) supplemented with 1 mM sodium pyruvate, 4 mM L-glutamine, or 5 mM beta-hydroxybutyrate (βHB) to measure the pyruvate-, glutamine-, or βHB-driven respiration. After measuring the basal respiration, 2 µM oligomycin, 4 µM carbonyl cyanide phenylhydrazone (FCCP), 5 μM UK5099 (#PZ0160, Sigma-Aldrich), and 2 μM rotenone/antimycin A were added sequentially. C2C12 cells were plated at the density of 10 000 cells per well for OCR assay.21 Pyruvate- and glutamine-driven respiration was measured using the same protocol as described above for fibroblasts, but the FCCP concentration was altered to $2 \mu M$. All OCR data were corrected for non-mitochondrial respiration. Cellular OCR and extracellular acidification rates (ECAR) were monitored in real time as measures of mitochondrial respiration and glycolysis, respectively.

2.10 | Statistical analysis

Data are expressed as mean \pm SD (SD). The non-paired Student's t test and one-way ANOVA were used to evaluate the statistical significance between experimental

TABLE 1 Features of patients with MPC1 variants

F1-I	ŀ	F2-I	F2-II	F2-III	F3-I	F3-II	Patient I ⁵	Patient II ^{2,16}	Patient III-1 ^{2,16}	Patient III-2 ^{2,16}
Consanguinity –		+	+	+	+	+	+	+	+	+
M		M	M	Н	Ţ	M	Ľ1	M	M	īŦ
5 m	u	3 m	After birth	After birth	6 mo	6 mo	After birth	After birth	NA	NA
5 y	5 y 7 mo	16 y 11 mo	12 y 7 mo	5 y 3 mo	8 y 9 mo	5 y 8 mo	Died at 19 mo	20 y	17 y	12 y
C.2l	c.208G > A; c.290G > A	c.109C > T	c.109C > T	c.109C > T	c.290G > A	c.290G > A	c.289C > T	c.236 T > A	c.236 T > A	c.236 T > A
p.A T P	p.Ala70Thr; p.Arg97Gln and p.Ala58Gfs*2	p.Pro37Ser	p.Pro37Ser	p.Pro37Ser	p.Arg97Gln and p.Ala58Glyfs*2	p.Arg97Gln and p.Ala58Glyfs*2	p.Arg97Trp and p.Ala58Glyfs*2	p.Leu79His	p.Leu79His	p.Leu79His
acial Mild dysmorphism	ld	Mild	Mild	Mild	I	I	+	NA	NA	NA
Microcephaly +		+	+	+	+	+	+	NA	NA	NA
Growth failure +		+	+	+	+	+	+	NA	NA	NA
+		+	+	I	1	1	+	+	NA	NA
Development + delay		+	+	+	+	+	+	+	+	+
Tra t	Transient convulsion + triggered by metabolic acidosis	+	I	I	I	I	I	+	NA	NA
Independently 5 y walking		2 y	1 y 10 mo	NA	2 y 6 mo	2 y	No walking at 16 mo NA	NA	NA	NA
Eye disorders Esc	Esotropia	I	Ī	Ī	L	Esotropia	Transient nystagmus and worsening visual contact	NA	Visual impairment	NA
I		+	+	NA	I	I	I	NA	NA	NA
1		+	+	+	1	1	ı	NA	NA	NA
High lactate in + serum		+	+	+	+	+	+	+	+	+
No	Normal	Normal	Elevated at birth	Normal	Elevated	Elevated	Normal	NA	NA	NA
No	Normal	NA	NA	NA	NA	NA	Normal	Normal	Normal	Normal (Continues)

Patient III-2 ^{2,16}	NA A	+
Patient III-1 ^{2,16}	N A	+
Patient II ^{2,16}	V V	+
Patient I ⁵	Cerebral atrophy with slight ventricular dilatation, periventricular leucomalacia and calcifications	+
F3-II	5 y 8 mo: Normal	I
F3-I	8 y 9 mo: Normal	I
F2-III	N	+
F2-II	8 y: Normal	+
F2-I	4 y: Brain atrophy. 13 y: Left temporal extra-axial CSF lesion, picture suggesting small arachnoid cyst.	+
F1-I	1 y: Bilateral symmetrical T2 signal hyperintensity at globus pallidus. 5 y: Hyperintensity signals at globus pallidus and suspicious high signals at thalamus.	+
	Brain MRI	Ketogenic diet +

TABLE 1 (Continued)

Abbreviations: +, Present; -, absent; GORD, gastro-oesophageal reflux disease; L, lactate; NA, not available; P, pyruvate.

**RefSer NM 0160984

groups. P < .05 was considered significant. GraphPad Prism 8 software was used to prepare graphs.

3 | RESULTS

3.1 | Clinical description

We enrolled six patients with MPC1 variants from three unrelated families, including four males and two females, aged from 5 to 16 years. Five affected individuals were from two consanguineous families. The essential clinical features of our patients compared with others are summarized in Table 1 (with additional information in supplementary material). Five of six patients were born at full term with one being born prematurely at 36-week gestation. Two patients presented in the immediate postnatal period (F2-II, III) with an age of onset in others of up to 6 months. The initial symptoms included developmental delay (F1-I, F3-I, and F3-II), gastro-oesophageal reflux disease (GORD; F2-I, II, and III), seizure (F2-I), transient tachypnoea and lactic acidosis (F2-II), and respiratory distress and feeding difficulties (F2-III). Global developmental delay, microcephaly, short stature, and poor weight gain were features common to all six patients. F1-I, F2-I, F2-II, and F2-III had mild facial dysmorphism. F2-I and F2-II had hearing loss; F1-I and F3-II had esotropia. The GORD and hearing loss observed in this cohort are clinical features not previously described in MPC1-related disease.

Elevated serum lactate was noted in all six patients. Increased serum pyruvate and a normal lactate/pyruvate ratio were observed in F1-I, but this information was not available for the other patients. Serum ammonia levels were elevated in F3-I and F3-II, transiently elevated in F2-II, and normal in F1-I, F2-I, and F2-III. All the patients had normal renal and liver function. Five patients had a cranial MRI performed, and subtle bilateral symmetrical T2 signal hyperintensity in globus pallidus and suspicious high signals at thalamus were identified in one of these patients (F1-I, Figure S1). This same patient exhibited developmental delay and elevated serum lactate and was therefore considered to have a Leigh-like syndrome (a manifestation of pathogenic MPC1 variants not previously recognized).22 Another patient had subtle brain atrophy with a small arachnoid cyst (F2-I), while the other three patients (F2-II, F3-I, and F3-II) had normal neuroimaging.

The ketogenic diet forces the body to utilize fat as its primary source of energy.²³ Based on the genetic finding of our patients, they had deficiency of pyruvate untaken, and ketone bodies can be the alternative fuel for OXPHOS; four of six patients were commenced on a

ketogenic diet (F1 and F2 members). And according to our experimental results described below, L-glutamine can substitute pyruvate to drive OCR on F1-I fibroblasts and ΔMPC1 C2C12 cells. L-glutamine is considered safe and is commonly used in China to treat children with gastrointestinal discomfort. After obtaining informed parental consent, two patients commenced L-glutamine 1 g/day (F1-I and F3-II). One month after commencing treatment with L-glutamine, F1-I exhibited improvement in drooling and his mother reported that he had begun to follow simple commands. After a further month, he was making his needs known using body language.

3.2 | Genetic analysis

Trio-WES performed on the patient and his parents of family 1 revealed the proband harboring compound heterozygous missense variants c.208G > A (p.Ala70Thr) and c.290G > A (p.Arg97Gln) in *MPC1* (RefSeq NM_016098.4). WES performed on the affected individuals of family 2 revealed a homozygous variant c.109C > T (p.Pro37Ser) in the same gene, segregating from the healthy family members. WES showed F3-I and F3-II carrying a homozygous c.290G > A (p.Arg97Gln) variant (Figure 1A-C). The three variants are novel variants that have not been reported

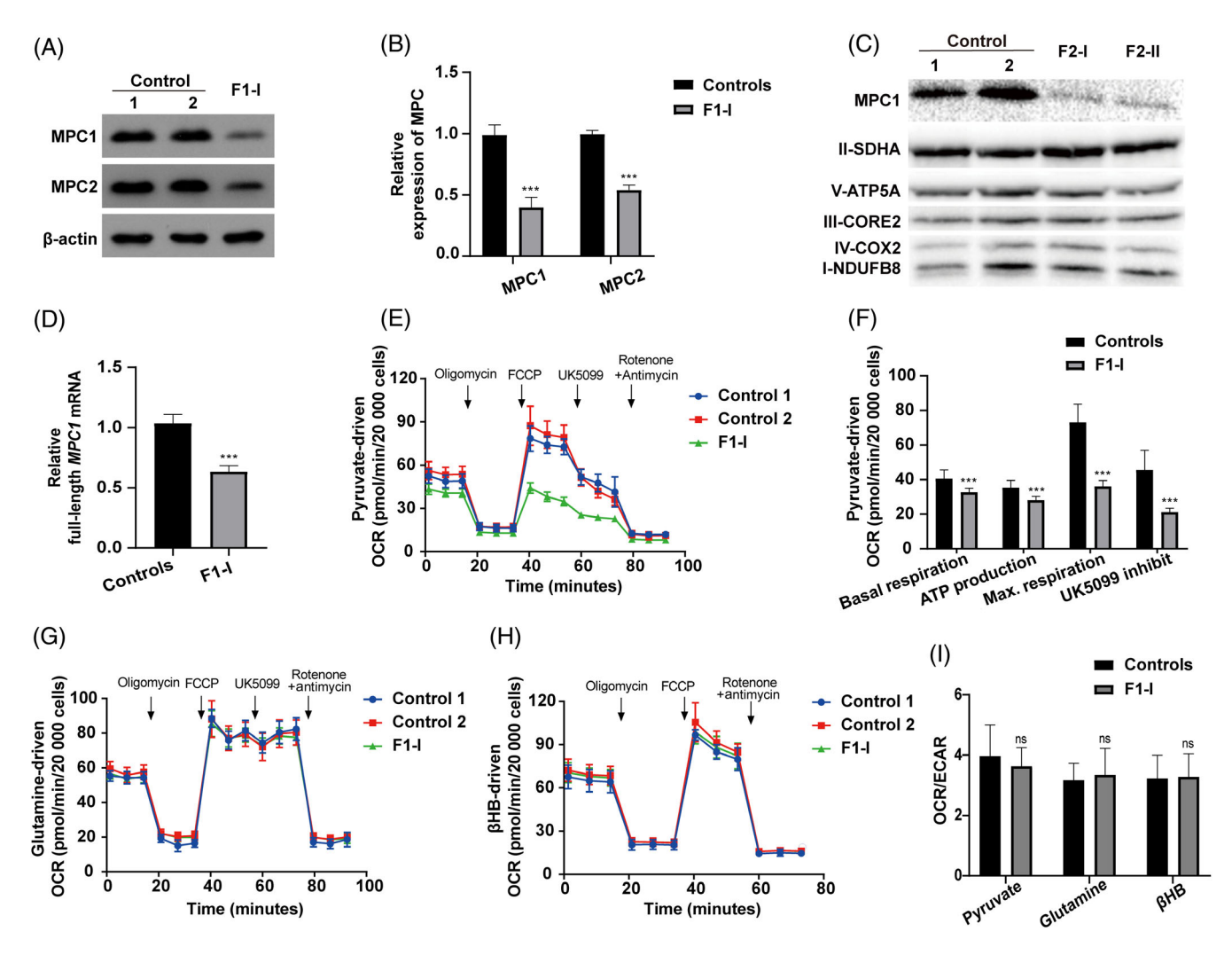


FIGURE 2 Analysis of MPC and OXPHOS protein levels, mRNA expression, and OCR in fibroblasts isolated from controls and patients (F1-1, F2-I/II). A, Western blot analysis of MPC1 and MPC2 protein expression from F1-I. Western blot is representative of at least three independent experiments. B, MPC1 and MPC2 protein levels of F1-I relative to those of β-actin. C, MPC1 and OXPHOS complex protein expression in F2. D, Relative full-length *MPC1* mRNA (primers targeting exon 4) expression level is quantified using qRT-PCR in controls and F1-I (n = 3). E-H, Overview of OCR driven by 1 mM pyruvate (E), 4 mM glutamine (G), and 5 mM βHB (H) in fibroblasts from F1-I as compared with controls (n = 14-16). F, Graphs of basal respiration, ATP production, maximal respiration, and UK5099 inhibited respiration calculated from OCR driven by 1 mM pyruvate. I, OCR/ECAR ratio for F1-I and controls under different substrates. Data are indicated as mean \pm SD. Significance is calculated using unpaired Student's *t* test. βHB, Beta-hydroxybutyrate; ECAR, extracellular acidification rates; FCCP, carbonyl cyanide phenylhydrazone; MPC, mitochondrial pyruvate carrier; ns = not significant; OCR, oxygen consumption rate. ****P < .001 (vs controls)

before. The variants were absent in the 1000 Genomes Project, ExAC, and gnomAD databases and were all rated pathogenic by several pathogenicity prediction tools (Table S2). Phylogenetic conservation analysis of the MPC1 proteins showed that all affected amino acids were highly conserved (Figure 1D). Electrophoresing MPC1 cDNA on agarose gel showed that apart from the expected band, there was a smaller band in the patient F1-I (Figure S2A). The cDNA fragments were purified from the gel and sequenced. The larger band of the patient contained c.208G > A (p.Ala70Thr) and c.290G > A (p. Arg97Gln) variants, corresponding to the full-length cDNA molecules with compound heterozygous variants. The smaller band carried the c.173_305del (p.Ala58Glyfs*2) variant, likely induced by the c.290G > A variant (Figure S2B and 1D). A similar double effect was determined for the c.289C > T variant reported by Bricker et al..² producing the p.Arg97Trp missense variant and the p.Ala58Glyfs*2 aberrant splicing variant, when exon 4 is spliced out.

3.3 | Decreased MPC expression and OCR in fibroblasts isolated from patients

MPC1 (F1-I, F2-I, and F2-II) and MPC2 (F1-I) expression was analysed in fibroblasts using western blotting. Cellular extracts from the patient exhibited significantly reduced protein levels of MPC1 in F1-I, F2-I, and F2-II, and MPC2 protein levels were also reduced in F1-I compared to healthy controls (Figure 2A-C). The decreased MPC1 levels in patients from family 2 indicate that the homozygous p.Pro37Ser is inducing protein instability. Relative transcript levels of MPC1 and MPC2 from F1-I were assessed using qRT-PCR. MPC1 mRNA analysis targeting exon 3 was used to identify the expression of all MPC1 transcripts (full-length transcripts with missense variants and truncated transcripts), while mRNA analysis targeting exon 4 was used to evaluate the full-length transcripts harboring missense variants (Figure 1D). The mRNA expression levels of total MPC1 and MPC2 were not significantly different from those of controls but that

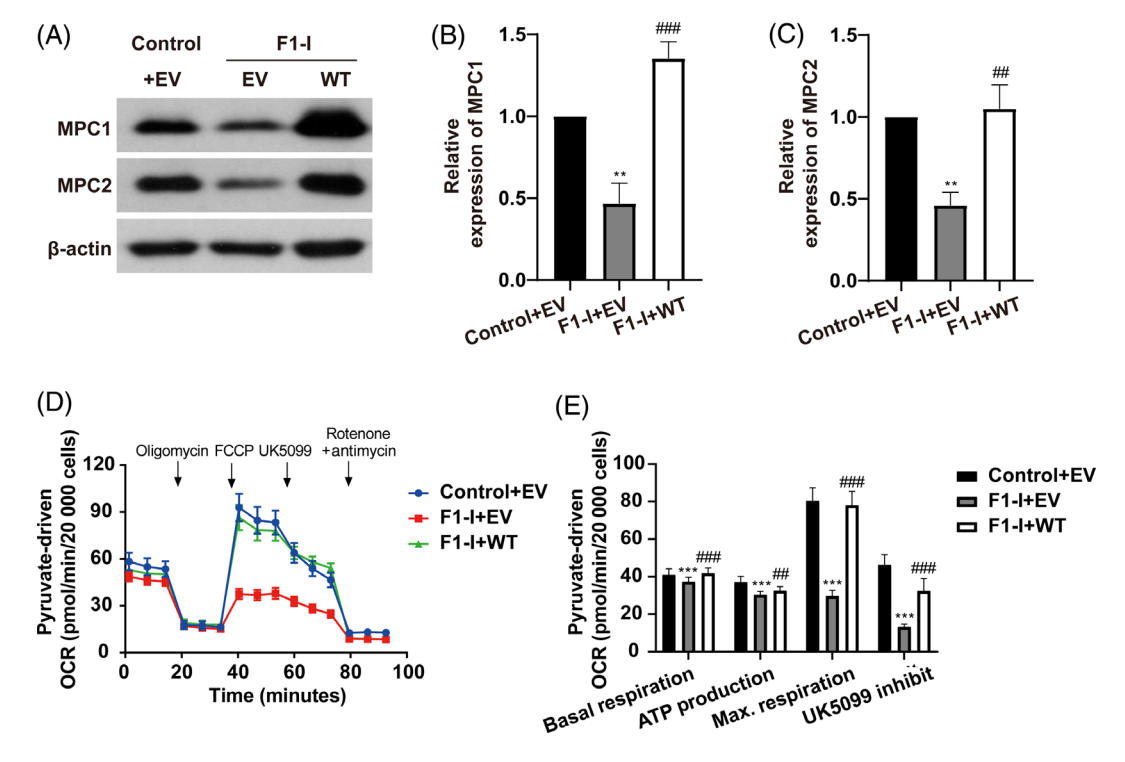


FIGURE 3 MPC protein level and OCR analyses in complemented F1-I fibroblasts and transduced control fibroblasts. A, Western blot analysis of MPC1 and MPC2 expression in control fibroblasts transduced with empty vectors (control + EV) and in F1-I fibroblasts complemented with EV (F1-I + EV) and human MPC1 WT (F1-I + WT; n=3). B and C, Quantitative analysis of MPC1 (B) and MPC2 (C) protein levels relative to β -actin in transduced control fibroblasts and complemented F1-I fibroblasts. D, Overview of OCR driven by 1 mM pyruvate in control and F1-I fibroblasts after transduction with the indicated vector (n=14-16). E, Graphs of basal respiration, ATP production, maximal respiration, and UK5099-inhibited respiration calculated from OCR data shown in (D). Data are indicated as mean \pm SD. Significance is calculated using unpaired Student's t test. EV, Empty vector; FCCP, carbonyl cyanide phenylhydrazone; OCR, oxygen consumption rate; WT, wild type. **P < .01 (vs control + EV); ***P < .01 (vs F1-I + EV); ***P < .01 (vs F1-I + EV); ***P < .01 (vs F1-I + EV)

of the full-length MPC1 mRNA was partially decreased (P < .001, Figure 2D and S3), suggesting that c.290G > A is mainly resulting in the aberrant splicing of exon 4 and to a much lesser extent in the missense variant p. Arg97Gln on the full transcript. Immunoblotting analysis of cultured-fibroblast lysates showed similar expression levels of OXPHOS complex subunits in patients (F1-I and F2-I/II) and controls (Figure 2C and S4).

Basal, maximal, adenosine triphosphate-linked, and UK5099-inhibited pyruvate-driven OCR were all significantly reduced in F1-I compared to controls (Figure 2E, F). UK5099, which acts as an MPC inhibitor, suppressed pyruvate transport into the mitochondrial matrix, decreasing respiration in controls but had no effect on patient fibroblasts. However, levels of glutamine- and β HB-driven respiration were similar between the case and controls (Figure 2G,H). The OCR/ECAR ratio in pyruvate-driven OCR, although not statistically significant, was a little lower in F1-I compared to controls. No statistically significant differences of OCR/ECAR were noted between the two groups in glutamine and β HB-

driven respiration (Figure 2I). The impaired mitochondrial pyruvate-driven respiration with normal glutamineand βHB-driven respiration indicated that the patient had a deficiency in utilizing pyruvate.

3.4 | Delivery of WT *MPC1* restored the impaired OCR in patient F1-I fibroblasts

To verify that the impaired mitochondrial respiration observed in patient F1-I fibroblasts was due to the loss of *MPC1* function, gene rescue experiments were performed. After transfection of F1-I fibroblasts with human *MPC1* WT cDNA, overexpression of MPC1 protein was observed in addition to an increase in MPC2 protein levels compared to control fibroblasts expressing empty vector (Figure 3A-C). Patient cells expressing *MPC1* WT demonstrated complete rescue of mitochondrial respiration driven by pyruvate, whereas the patient cells expressing empty vector still showed impaired pyruvate-driven respiration (Figure 3D,E).

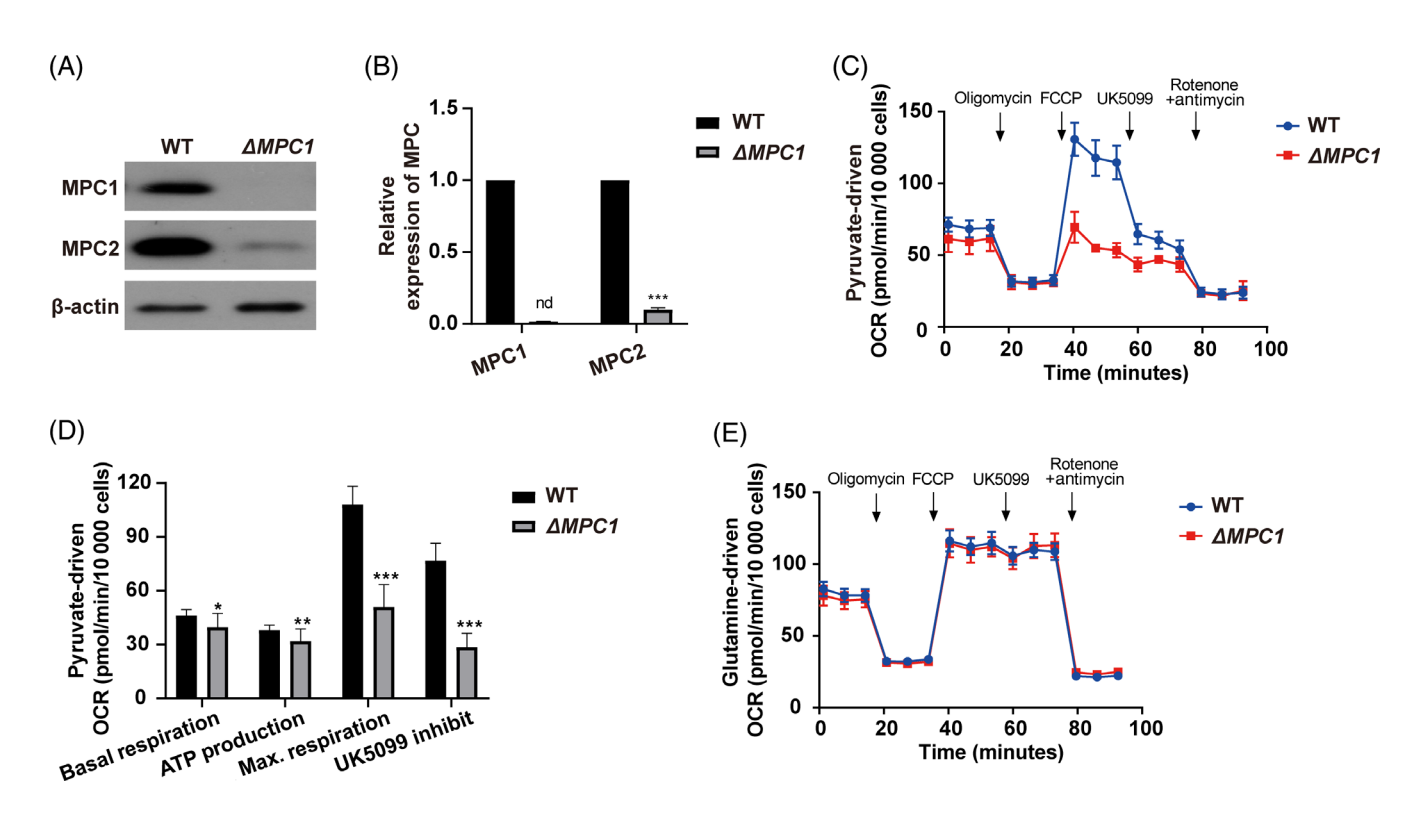


FIGURE 4 Generation and characterization of *MPC1* knockout C2C12 cell lines ($\Delta MPC1$). A, Western blot analysis of MPC1 and MPC2 protein expression in WT C2C12 cells (WT) and $\Delta MPC1$ cells. β-actin is used as a loading control (n = 3). B, MPC1 and MPC2 protein levels relative to those of β-actin in WT and $\Delta MPC1$ cells (n = 3). C and E, Overview of OCR driven by 1 mM pyruvate (C) and 4 mM glutamine (E) in $\Delta MPC1$ cells as compared with that in WT cells (n = 14-16). D, Graphs of basal respiration, ATP production, maximal respiration, and UK5099-inhibited respiration calculated from OCR driven by 1 mM pyruvate. Data are indicated as mean ± SD. Significance calculated by unpaired Student's *t* test. FCCP, Carbonyl cyanide phenylhydrazone; nd = not detected (vs WT); OCR, oxygen consumption rate; WT, wild type. *P < .05; **P < .05; **P < .01; ***P < .001

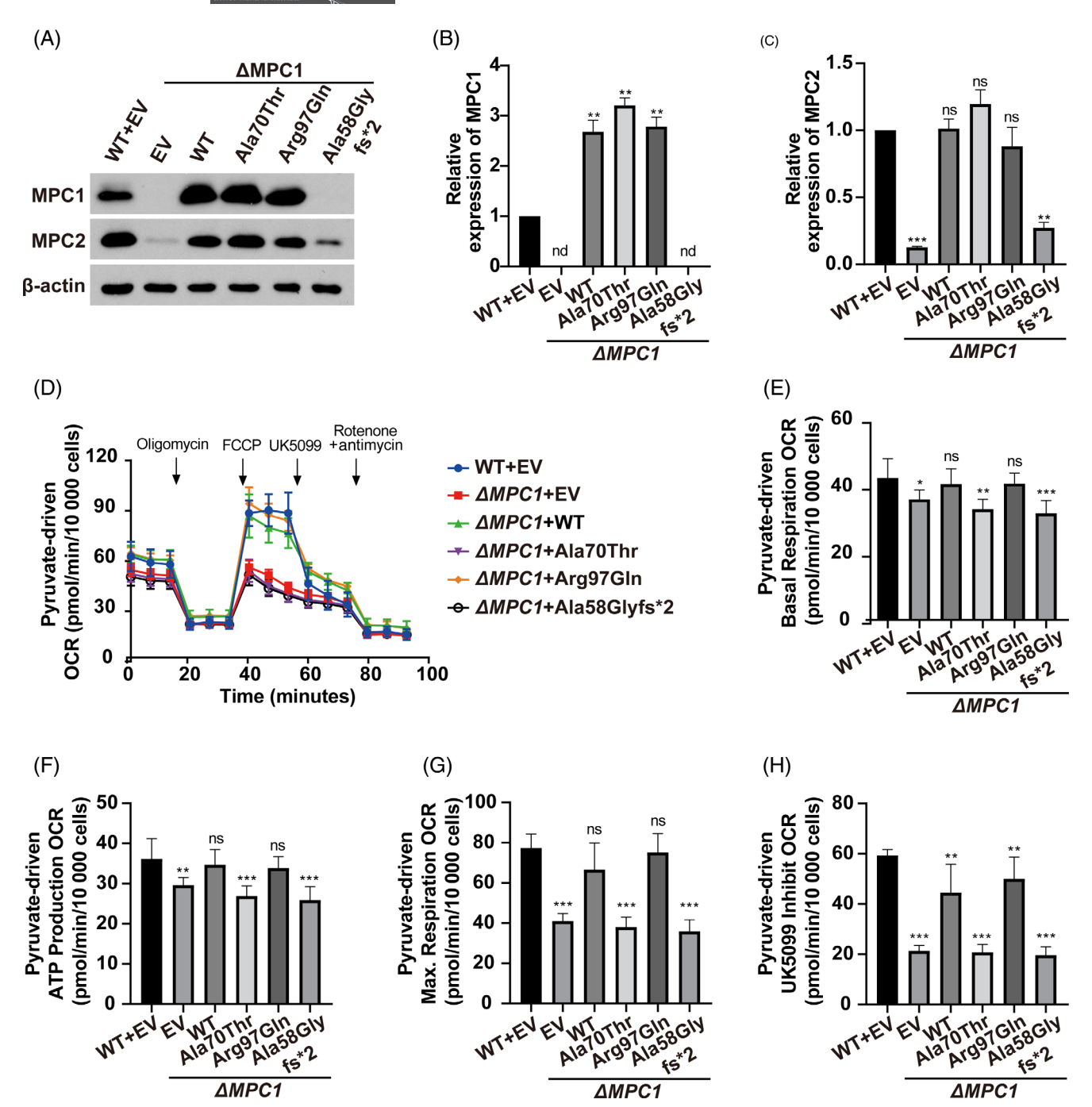


FIGURE 5 *MPC1* patient variants display impaired MPC complex stability or function. A, Western blot analysis of MPC1 and MPC2 protein expression in WT C2C12 cells transduced with empty vector (WT + EV) compared with those in Δ*MPC1* cells complemented with empty vector (Δ*MPC1* + EV), human *MPC1* WT (Δ*MPC1* + WT), and *MPC1* mutant vectors (Δ*MPC1* + Ala70Thr, Δ*MPC1* + Arg97Gln, Δ*MPC1*+ Ala58Glyfs*2; n = 3). B and C, MPC1 (B) and MPC2 (C) protein levels relative to β-actin. D, OCR driven by 1 mM pyruvate in WT and Δ*MPC1* cells after transfection with the indicated vector (n = 14-16). E-H, Graphs of basal respiration (E), ATP production (F), maximal respiration (G), and UK5099-inhibited respiration (H) calculated from OCR data shown in (D). Data indicated as mean ± SD. Significance calculated by one-way ANOVA. EV, Empty vector; FCCP, carbonyl cyanide phenylhydrazone; nd = not detected (vs WT + EV); ns = not significant; OCR, oxygen consumption rate; WT, wild type. *P < .05; **P < .05; **P < .01; ***P < .001

3.5 | Modeling of *MPC1* variants in C2C12 cells

To analyse the mechanism by which the variants decrease MPC function, C2C12 cells were used for gene knockout and

subsequent complementation experiments. The $\Delta MPC1$ cells were generated using CRISPR/Cas9 and confirmed using western blot. Compared with WT cells, the $\Delta MPC1$ cells showed undetectable levels of MPC1 and only mild MPC2 protein expression during overexposure (Figure 4A,B).

 $\Delta MPC1$ cells showed strongly impaired pyruvate-driven respiration, but glutamine-driven respiration was similar to WT cells (Figure 4C-E). The cDNAs harboring the WT, Ala70Thr, Arg97Gln, and Ala58Glyfs*2 alleles of human MPC1 were expressed individually into $\Delta MPC1$ cells. After two rounds of puromycin treatment, all surviving cells were successfully employed as variant models.

3.6 | Patient MPC1 variants affect MPC complex stability and mitochondrial respiration differently

Western blot analysis was performed to measure MPC1 and MPC2 expression levels in cells transfected with the plasmids of interest. ΔMPC1 cells expressing the MPC1 WT, Ala70Thr, and Arg97Gln constructs showed high quantities of MPC1 and normal levels of MPC2, whereas cells expressing truncated Ala58Glyfs*2 displayed undetectable MPC1 and decreased MPC2 levels (Figure 5A-C).

The OCR assay was utilized to measure the effect of variants on mitochondrial respiration. $\Delta MPC1$ cells expressing MPC1 WT and Arg97Gln restored pyruvate-driven respiration to native levels. When compared to WT C2C12 cells, the Ala70Thr and Ala58Glyfs*2 constructs failed to rescue FCCP-stimulated respiration driven by pyruvate in $\Delta MPC1$ cells (Figure 5D-H). Taken together, MPC1 Ala58Glyfs*2 is a truncated protein that results in unstable MPC1 expression and has an inability to form MPC complex. The MPC1 Ala70Thr variant stabilized the MPC complex but lost the ability to carry pyruvate into the mitochondrion. The overexpression of Arg97Gln retained nearly normal MPC complex function, which suggests that the c.290G > A variant is exerting its pathogenicity mainly through the aberrant splicing effect. This interpretation is also supported by the qPCR data showing markedly decreased full-length MPC1 mRNA in patient F1-I, indicating that the aberrant splicing effect of c.290G > A is more prominent.

4 | DISCUSSION

MPC1-related mitochondrial disease is a rare autosomal recessive inherited disease in which global developmental delay, microcephaly, and failure to survive have been reported previously in a small number of patients.^{2,5} Here, we report six cases due to novel *MPC1* variants, identifying GORD, hearing loss, and a Leigh-like presentation as novel clinical features within this patient cohort. While the affected individual reported by Brivet and colleagues⁵ had impaired renal, cardiac, and liver functions,

we do not observe this in our cohort of patients. Elevated levels of serum lactate, with a normal lactate/pyruvate ratio, are clues to a diagnosis of a pyruvate-related metabolic deficiency, and a normal pyruvate dehydrogenase complex (PDHc) activity helps distinguish MPC deficiency from PDHc deficiencies. Cranial MRI in patients with MPC1 variants is unremarkable, though one of our patients showed subtle bilateral symmetric lesions of globus pallidus and suspicious high signals at thalamus. In the context of clinical features of developmental delay and elevated serum lactate, this patient was subsequently diagnosed with a Leigh-like syndrome, a previously unreported clinical presentation for patients with pathogenic MPC1 variants. To date, this is the second detailed clinical report involving novel variants in MPC1, though the number of reported patients remains very limited and we are unable to identify any common phenotypegenotype relationships in MPC deficiency.

Several results support the pathogenicity of MPC1 variants identified in our patient cohort. Firstly, variants observed in our patients were absent in the 1000 Genomes Project, ExAC, and gnomAD databases; were predicted as pathogenic by several prediction software packages; and the affected amino acids were highly conserved across species. Secondly, variants present in affected patients from the three families with similar clinical phenotypes segregated with disease in those families, that is, no healthy family members harboured bi-allelic variants. Thirdly, western blot showed decreased MPC1 and MPC2 protein expression in patients. Fourthly, impaired pyruvate-driven respiration was restored by lentiviral-mediated expression of MPC1 WT cDNA, whereas glutamine- and βHB-driven respiration was normal in patient F1-I fibroblasts. Finally, complementation with homozygous mutant cDNA in ΔMPC1 C2C12 cells further showed that p.Ala70Thr and p.Ala58Glyfs*2 variants impair pyruvate-driven respiration, with p.Ala58Glyfs*2 also affecting the MPC complex stability. The pathogenicity of p.Arg97Gln is disputable.

Complementation of *MPC1* p.Ala70Thr cDNA into Δ*MPC1* cells resulted in a stable MPC1 and endogenous MPC2 expression levels, but the cells lacked the ability to use pyruvate as a substrate to drive mitochondrial respiration. *MPC1* Ala70 is located in the second transmembrane domain, and nearby amino acids Gly74 and Pro75 are predicted to form hinges and provide structural flexibility facilitating Arg76 rotation. ²⁴ The MPC1 C-terminus is essential for MPC1 stability; C-terminal truncations of more than 12 amino acids are severely destabilizing. ¹⁶ The Ala58Glyfs*2 truncated protein is predicted to contain 60 amino acids instead of the original 109 amino acids, which results in undetectable MPC1 protein and unstable

MPC complex. Complementation of $\Delta MPC1$ cells with p. Arg97Gln cDNA led to overexpression of MPC1 and recovered MPC2 stability, thus restoring FCCP-stimulated respiration to near-normal levels. Haploinsufficiency may be the cause of MPC dysfunction in patients with this variant. The p.Pro37Ser variant decreased the expression of MPC1, thus resulting in an unstable MPC complex. These data demonstrate that the variants from our patients are loss of function, and they result in an unstable MPC1 protein or a stable MPC complex that inefficiently carries pyruvate into the mitochondrial matrix.

Previous studies demonstrated that many metabolic pathways compensated for the loss of MPC function, making replacement therapy possible. 25,26 Pyruvatealanine cycling can potentially compensate for the loss of MPC function. Alanine transamination regulates the flux of pyruvate carbon into the TCA cycle in liverspecific deletion of MPC2 hepatocytes.²⁷ Fibroblasts of F1-I had a slightly lower OCR/ECAR ratio when pyruvate was used as fuel for energy generation and were not fully reliant on glycolysis. An MPC1 knockout mouse displays embryonic lethality while feeding pregnant dams with a ketogenic diet allowed normal gestation and development of MPC-deficient pups. 28 In addition, ketone bodies have been shown to promote mitochondrial biogenesis and increase complex I activity. 23,29 Eight patients tried early introduction of a ketogenic diet, and while the first reported patient died at 19 months, others survived, albeit with different degrees of developmental delay.⁵ According to our experimental results, MPC1 variants did not influence glutamine- or βHB-driven respiration, rendering glutamine and βHB as an alternative substrate for TCA cycle and energy generation. A ketogenic diet has been widely used in pyruvate metabolic disorders, whereas glutamine has not been previously considered as a treatment for this deficiency. Impaired mitochondrial pyruvate transporting activates glutamate dehydrogenase and reroutes glutamine metabolism to generate both oxaloacetate and acetyl-CoA, enabling persistent TCA cycle function.³⁰ Considering glutamine is a versatile amino acid commonly used in gastrointestinal diseases and was approved by the Food and Drug Administration to prevent acute complications in sickle cell anaemia in 2017,³¹ we provided supplemental glutamine to patient F1-I. No side effects were reported in our patient after administering glutamine for 3 months, but efficacy remains difficult to assess at this early stage. If this glutamine therapy proves successful, we would suggest commencing treatment as early as possible to avoid the adverse impact of pyruvate deficiency on brain development.

In conclusion, our study provides a new insight into MPC deficiency and illustrates that Leigh-like syndrome may be a clinical presentation of pathogenic MPC1 variants. In addition, we propose that L-glutamine and βHB could be potential therapies for MPC deficiency though they require further rigorous clinical studies to demonstrate clinical effectiveness.

CONFLICT OF INTEREST

The authors declare that they have no conflict of interest.

AUTHOR CONTRIBUTIONS

All authors approved the final content of the manuscript. Huafang Jiang: Writing - original manuscript; final manuscript approval; functional experiments to explore pathogenicity. Ahmad Alahmad: Writing - original manuscript; final manuscript approval; clinical work; functional experiments to explore pathogenicity. Robert W. Taylor: Writing - original manuscript; final manuscript approval; clinical work. Robert McFarland: Writing - original manuscript; final manuscript approval; clinical work. Fang Fang: Writing - original manuscript; final manuscript approval; study conception, design, and supervision; writing - review and editing. Xiaoling Fu: Clinical work. Xiaodi Han: Clinical work. Tianyu Song: Clinical work. Buthaina Albash: Clinical work. Ahmad Alageel: Clinical work. Holger Prokisch: Clinical work; writing - review and editing. Zhimei Liu: Genetic analysis. Manting Xu: Genetic analysis. Junling Wang: Fibroblast studies. Song Fu: Functional experiments to explore pathogenicity. Lanlan Li: Functional experiments to explore pathogenicity. Shanshan Liu: Functional experiments to explore pathogenicity. Vasilescu Catalina: Writing – review and editing.

ANIMAL RIGHTS

This article does not contain any studies with animal subjects performed by any of the authors.

ETHICS STATEMENT

All procedures followed were in accordance with the ethical standards of the responsible committee on human experimentation (institutional and national) and with the Helsinki Declaration of 1975, as revised in 2000. Informed consent was obtained from all patients for being included in the study. "Molecular genetic diagnosis and pathogenesis of mitochondrial diseases" (2017-k-60) was approved by the Ethics Committee of Beijing Children's hospital. The recruitment of patients for research of Mitochondrial Disease in Kuwait was approved by the Ethics Committee at the Kuwait Medical Genetics Centre in 2017. Consent

from patients and their guardians in China and Kuwait were obtained for diagnostic and research purposes.

PATIENT CONSENT FOR PUBLICATION Obtained

ORCID

Huafang Jiang https://orcid.org/0000-0002-6632-1793

Ahmad Alahmad https://orcid.org/0000-0001-9754-2532

Zhimei Liu https://orcid.org/0000-0003-0393-7598

Manting Xu https://orcid.org/0000-0002-3155-4810

Holger Prokisch https://orcid.org/0000-0003-2379-6286

Robert W. Taylor https://orcid.org/0000-0002-7768-8873

Robert McFarland https://orcid.org/0000-0002-8833-2688

Fang Fang https://orcid.org/0000-0001-6362-7896

REFERENCES

- 1. McCommis KS, Finck BN. Mitochondrial pyruvate transport: a historical perspective and future research directions. *Biochem J.* 2015;466(3):443-454.
- 2. Bricker DK, Taylor EB, Schell JC, et al. A mitochondrial pyruvate carrier required for pyruvate uptake in yeast, drosophila, and humans. *Science*. 2012;337(6090):96-100.
- Herzig S, Raemy E, Montessuit S, et al. Identification and functional expression of the mitochondrial pyruvate carrier. *Science*. 2012;337(6090):93-96.
- Vanderperre B, Bender T, Kunji ER, Martinou JC. Mitochondrial pyruvate import and its effects on homeostasis. *Curr Opin Cell Biol*. 2015;33:35-41.
- 5. Brivet M, Garcia-Cazorla A, Lyonnet S, et al. Impaired mitochondrial pyruvate importation in a patient and a fetus at risk. *Mol Genet Metab.* 2003;78(3):186-192.
- 6. Wang K, Li M, Hakonarson H. ANNOVAR: functional annotation of genetic variants from high-throughput sequencing data. *Nucleic Acids Res.* 2010;38(16):e164.
- 7. 1000 Genomes Project Consortium, Abecasis GR, Auton A, et al. An integrated map of genetic variation from 1,092 human genomes. *Nature*. 2012;491(7422):56-65.
- 8. Karczewski KJ, Francioli LC, Tiao G, et al. The mutational constraint spectrum quantified from variation in 141,456 humans. *Nature*. 2020;581(7809):434-443.
- Lek M, Karczewski KJ, Minikel EV, et al. Analysis of proteincoding genetic variation in 60,706 humans. *Nature*. 2016;536(7616): 285-291.
- Ng PC, Henikoff S. SIFT: predicting amino acid changes that affect protein function. Nucleic Acids Res. 2003;31(13):3812-3814.
- 11. Adzhubei I, Jordan DM, Sunyaev SR. Predicting functional effect of human missense mutations using PolyPhen-2. *Curr Protoc Hum Genet*. 2013;7(Unit7):20.
- 12. Schwarz JM, Rodelsperger C, Schuelke M, Seelow D. MutationTaster evaluates disease-causing potential of sequence alterations. *Nat Methods*. 2010;7(8):575-576.

- 13. Rentzsch P, Witten D, Cooper GM, Shendure J, Kircher M. CADD: predicting the deleteriousness of variants throughout the human genome. *Nucleic Acids Res.* 2019;47(D1):D886-D894.
- Choi Y, Chan AP. PROVEAN web server: a tool to predict the functional effect of amino acid substitutions and indels. *Bioinformatics*. 2015;31(16):2745-2747.
- Richards S, Aziz N, Bale S, et al. Standards and guidelines for the interpretation of sequence variants: a joint consensus recommendation of the American College of Medical Genetics and Genomics and the Association for Molecular Pathology. *Genet Med.* 2015;17(5):405-424.
- Oonthonpan L, Rauckhorst AJ, Gray LR, Boutron AC, Taylor EB. Two human patient mitochondrial pyruvate carrier mutations reveal distinct molecular mechanisms of dysfunction. *JCI Insight*. 2019;5(13):e126132.
- Shalem O, Sanjana NE, Hartenian E, et al. Genome-scale CRISPR-Cas9 knockout screening in human cells. *Science*. 2014; 343(6166):84-87.
- 18. Gibson DG, Young L, Chuang RY, Venter JC, Hutchison CA 3rd, Smith HO. Enzymatic assembly of DNA molecules up to several hundred kilobases. *Nat Methods*. 2009;6(5):343-345.
- Dull T, Zufferey R, Kelly M, et al. A third-generation lentivirus vector with a conditional packaging system. *J Virol.* 1998;72(11):8463-8471.
- Kremer LS, Prokisch H. Identification of disease-causing mutations by functional complementation of patient-derived fibroblast cell lines. *Methods Mol Biol.* 2017;1567;391-406.
- 21. Nicholls DG, Darley-Usmar VM, Wu M, Jensen PB, Rogers GW, Ferrick DA. Bioenergetic profile experiment using C2C12 myoblast cells. *J Vis Exp.* 2010;46:2511.
- Baertling F, Rodenburg RJ, Schaper J, et al. A guide to diagnosis and treatment of Leigh syndrome. J Neurol Neurosurg Psychiatry. 2014;85(3):257-265.
- 23. Vidali S, Aminzadeh S, Lambert B, et al. Mitochondria: the ketogenic diet—A metabolism-based therapy. *Int J Biochem Cell Biol.* 2015;63:55-59.
- Lee J, Jin Z, Lee D, Yun JH, Lee W. Characteristic analysis of homo- and heterodimeric complexes of human mitochondrial pyruvate carrier related to metabolic diseases. *Int J Mol Sci.* 2020;21(9): 3403.
- Bender T, Martinou JC. The mitochondrial pyruvate carrier in health and disease: to carry or not to carry? *Biochim Biophys Acta*. 2016;1863(10):2436-2442.
- 26. Vacanti NM, Divakaruni AS, Green CR, et al. Regulation of substrate utilization by the mitochondrial pyruvate carrier. *Mol Cell*. 2014;56(3):425-435.
- 27. McCommis KS, Chen Z, Fu X, et al. Loss of mitochondrial pyruvate carrier 2 in the liver leads to defects in gluconeogenesis and compensation via pyruvate-alanine cycling. *Cell Metab*. 2015;22(4):682-694.
- 28. Vanderperre B, Herzig S, Krznar P, et al. Embryonic lethality of mitochondrial pyruvate carrier 1 deficient mouse can be rescued by a ketogenic diet. *PLoS Genet*. 2016;12(5): e1006056.
- 29. Hughes SD, Kanabus M, Anderson G, et al. The ketogenic diet component decanoic acid increases mitochondrial citrate synthase and complex I activity in neuronal cells. *J Neurochem*. 2014;129(3):426-433.

- 30. Yang C, Ko B, Hensley CT, et al. Glutamine oxidation maintains the TCA cycle and cell survival during impaired mitochondrial pyruvate transport. *Mol Cell*. 2014;56(3):414-424.
- 31. Niihara Y, Miller ST, Kanter J, et al. A phase 3 trial of l-glutamine in sickle cell disease. *N Engl J Med.* 2018;379(3):226-235.

SUPPORTING INFORMATION

Additional supporting information may be found in the online version of the article at the publisher's website.

How to cite this article: Jiang H, Alahmad A, Fu S, et al. Identification and characterization of novel *MPC1* gene variants causing mitochondrial pyruvate carrier deficiency. *J Inherit Metab Dis*. 2022;1-14. doi:10.1002/jimd.12462